

Role of Thylakoid ATP/ADP Carrier in Photoinhibition and Photoprotection of Photosystem II in Arabidopsis^{1[W][OA]}

Lan Yin, Björn Lundin², Martine Bertrand, Markus Nurmi, Katalin Solymosi, Saijaliisa Kangasjärvi, Eva-Mari Aro, Benoît Schoefs, and Cornelia Spetea*

Division of Molecular Genetics, Department of Physics, Chemistry, and Biology, Linköping University, 581 83 Linköping, Sweden (L.Y., B.L., C.S.); National Institute for Marine Sciences and Techniques, Cnam, 50103 Cherbourg-Octeville cedex, France (M.B.); Department of Plant Anatomy, Eötvös University, 1117 Budapest, Hungary (K.S.); Department of Biochemistry and Food Chemistry, University of Turku, 20014 Turku, Finland (M.N., S.K., E.-M.A.); and UMR Plante-Microbe-Environnement, INRA-1088/CNRS-5184/Université de Bourgogne, 21065 Dijon cedex, France (B.S.)

The chloroplast thylakoid ATP/ADP carrier (TAAC) belongs to the mitochondrial carrier superfamily and supplies the thylakoid lumen with stromal ATP in exchange for ADP. Here, we investigate the physiological consequences of TAAC depletion in Arabidopsis (*Arabidopsis thaliana*). We show that the deficiency of TAAC in two T-DNA insertion lines does not modify the chloroplast ultrastructure, the relative amounts of photosynthetic proteins, the pigment composition, and the photosynthetic activity. Under growth light conditions, the mutants initially displayed similar shoot weight, but lower when reaching full development, and were less tolerant to high light conditions in comparison with the wild type. These observations prompted us to study in more detail the effects of TAAC depletion on photoinhibition and photoprotection of the photosystem II (PSII) complex. The steady-state phosphorylation levels of PSII proteins were not affected, but the degradation of the reaction center II D1 protein was blocked, and decreased amounts of CP43-less PSII monomers were detected in the mutants. Besides this, the mutant leaves displayed a transiently higher nonphotochemical quenching of chlorophyll fluorescence than the wild-type leaves, especially at low light. This may be attributed to the accumulation in the absence of TAAC of a higher electrochemical H⁺ gradient in the first minutes of illumination, which more efficiently activates photoprotective xanthophyll cycle-dependent and independent mechanisms. Based on these results, we propose that TAAC plays a critical role in the disassembly steps during PSII repair and in addition may balance the trans-thylakoid electrochemical H⁺ gradient storage.

In plants, the chloroplast thylakoid membrane is the site of light-driven photosynthetic reactions coupled to ATP synthesis. There are four major protein complexes involved in these reactions, namely, PSI, PSII, the

cytochrome *b₆f*, and the H⁺-translocating ATP synthase (for review, see Nelson and Ben-Shem, 2004). The photosystems and the cytochrome *b₆f* complex also contain redox components and pigments bound to protein subunits. Their synthesis, assembly, optimal function, and repair during normal development and stress require a number of transport and regulatory mechanisms. In this context, the water-oxidizing PSII complex composed of more than 25 integral and peripheral proteins attracts special attention since its reaction center D1 subunit is degraded and replaced much faster than the other subunits under excess and even growth light conditions (for review, see Aro et al., 2005). Thus, the D1 protein turnover is the major event in the repair cycle of the PSII complex and occurs subsequently to the inactivation of PSII electron transport. D1 degradation is most likely performed by thylakoid FtsH and Deg proteases, operating on both sides of the thylakoid membrane (Lindahl et al., 2000; Haussühl et al., 2001; Silva et al., 2003; Kapri-Pardes et al., 2007). The PSII repair cycle is regulated by reversible phosphorylation of several core subunits (Tikkanen et al., 2008).

¹ This work was supported by grants from the Swedish Research Council, the Swedish Research Council for Environment, Agriculture, and Space Planning (Formas), the Graduate Research School in Genomics and Bioinformatics (C.S.), the Academy of Finland (to E.-M.A.), the French Ministère de l'Éducation Nationale de l'Enseignement Supérieur et de la Recherche, and the Institut National de la Recherche Agronomique, the Centre National de la Recherche Scientifique (B.S.).

² Present address: Graduate School of Natural Science and Technology, Okayama University, 700-8530 Okayama, Japan.

* Corresponding author; e-mail corssp@ifm.liu.se.

The author responsible for distribution of materials integral to the findings presented in this article in accordance with the policy described in the Instructions for Authors (www.plantphysiol.org) is: Cornelia Spetea (corssp@ifm.liu.se).

[W] The online version of this article contains Web-only data.

[OA] Open Access articles can be viewed online without a subscription.

www.plantphysiol.org/cgi/doi/10.1104/pp.110.155804

ATP is produced as a result of the light-driven photosynthetic reactions in the thylakoid membrane and mainly is utilized in the carbon fixation reactions occurring in the soluble stroma. Besides this, ATP also drives several energy-dependent processes occurring on the stromal side of the thylakoid membrane, including phosphorylation, folding, import, and degradation of proteins. Furthermore, experimental evidence for ATP transport across the thylakoid membrane and nucleotide metabolism inside the luminal space has been reported (Spetea et al., 2004; for review, see Spetea and Thuswaldner, 2008; Spetea and Schoefs, 2010). The protein responsible for the thylakoid ATP transport activity has been identified in Arabidopsis (*Arabidopsis thaliana*) as the product of the At5g01500 gene and functionally characterized in *Escherichia coli* as an ATP/ADP exchanger (Thuswaldner et al., 2007). This protein is homologous to the extensively studied bovine mitochondrial ADP/ATP carrier and therefore has been named thylakoid ATP/ADP carrier (TAAC). In the same report, it has been demonstrated that TAAC transports ATP from stroma to lumen in exchange for ADP, as based on radioactive assays using thylakoids isolated from Arabidopsis wild-type plants and a T-DNA insertion knockout line (named *taac*). Furthermore, TAAC was shown to be mainly expressed in photosynthetic tissues with an up-regulation during greening, senescence, and stress (e.g. high light) conditions, implying a physiological role during thylakoid biogenesis and turnover.

The ATP translocated by TAAC across the thylakoid membrane is converted to GTP by the luminal nucleoside diphosphate kinase III; GTP can then be bound and hydrolyzed to GDP and inorganic phosphate by the PsbO protein, a luminal extrinsic subunit of the PSII complex (Spetea et al., 2004; Lundin et al., 2007a). The anion transporter 1 from Arabidopsis has been proposed to export to the stroma the phosphate generated during nucleotide metabolism in the thylakoid lumen (Ruiz Pavón et al., 2008). Between the two PsbO isoforms in Arabidopsis, it has recently been reported that PsbO2 plays an essential role in D1 protein turnover during high light stress and that it has a higher GTPase activity than PsbO1 (Lundin et al., 2007b, 2008; Allahverdiyeva et al., 2009). The precise mechanism of PsbO2-mediated PSII repair is not known. Nevertheless, the requirement of GTP for efficient proteolytic removal of the D1 protein during repair of photoinactivated PSII was previously reported (Spetea et al., 1999). Furthermore, it has been proposed that the PsbO2 type of PSII complexes undergo more efficient repair. This has been attributed to the PsbO2-mediated GTPase activity that induces PsbO2 release from the complex, thus facilitating the next steps in the repair process, namely, dissociation of the CP43 subunit and proteolysis of the D1 subunit (Lundin et al., 2007b, 2008).

TAAC may represent the missing link between ATP synthesis on the stromal side of the thylakoid membrane and nucleotide-dependent reactions in the lu-

menal space. The *taac* mutant provides an interesting tool to study whether there are any regulatory networks between the activity of TAAC and PSII repair. Based on phenotypic characterization of two different T-DNA insertion lines of the TAAC gene, we report in this article that the PSII repair cycle is malfunctioning in the absence of TAAC and that the thermal photoprotection is faster activated during light stress.

RESULTS

PSII Activity under Growth Light Conditions

The *taac* knockout mutant, initially characterized by Thuswaldner et al. (2007), was obtained from the Institut National de la Recherche Agronomique Public-Lines collection (FLAG_443D03, Wassilewskija [Ws] ecotype) and is shown here to contain a single T-DNA insertion (Supplemental Fig. S1). A second homozygous *taac* mutant identified from Syngenta T-DNA insertion lines collection (SAIL_209_A12, Columbia ecotype) is described in Supplemental Figure S2.

At an irradiance of 120 $\mu\text{mol photons m}^{-2} \text{s}^{-1}$ (GL), the *taac* mutants grew initially with the same rate as the wild-type plants of the respective ecotype, but then slower and had significantly less (20%) leaf biomass compared to the wild type (Fig. 1, A and B; Supplemental Fig. S3, A and B). When examined with electron microscopy, structurally normal chloroplasts containing starch grains and thylakoid membranes with typical stacked grana were found in all types of plants (Fig. 1C; Supplemental Fig. S3C). Plastid length and width ranged in all samples between 5 to 6 and 2 to 3 μm , respectively. The studied plastid profiles contained 58 to 61 grana on average, and there was no large difference between *taac* and wild-type plants in this respect. Similarly, no large difference was found in height (number of appressed thylakoid lamellae per granum) or length of the grana between the mutants and their respective ecotypes. This indicates that depletion of TAAC does not influence chloroplast and thylakoid ultrastructure under average, nonstressful conditions.

The chlorophyll (Chl) content of whole leaves (expressed per leaf fresh weight or per leaf surface unit) and Chl *a/b* ratio were not significantly affected by the deficiency of TAAC in the mutant compared to the wild type (Table I; Supplemental Table S1). The maximum quantum yield of PSII photochemistry was the same in wild-type and *taac* leaves ($F_v/F_m = 0.8$). Similar steady-state rates of oxygen evolution were measured in thylakoid membranes in the presence of the PSII acceptor phenyl-*p*-benzoquinone. Nevertheless, addition of NH_4Cl has resulted in significantly higher rates of oxygen evolution in the mutant compared with the wild type. The observed difference is consistent with the existence in the mutant of an overall higher capacity for PSII electron transport per unit Chl. A stimulatory effect of NH_4Cl on the electron transport

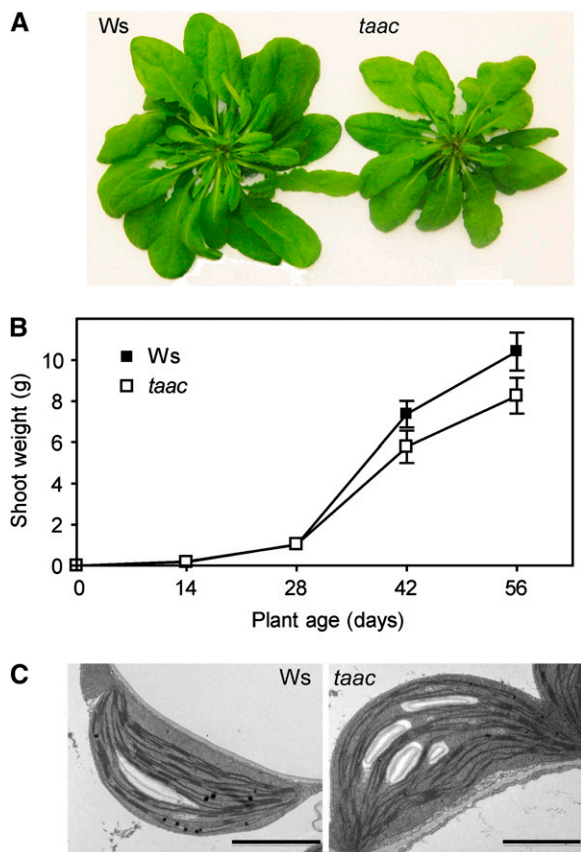


Figure 1. Comparison of the *taac* mutant with wild-type *Arabidopsis* plants of the same *Ws* ecotype. **A**, The photographs of representative plants were taken at an age of 42 d of growth using a hydroponic system at an irradiance of $120 \mu\text{mol photons m}^{-2} \text{s}^{-1}$. **B**, Plot of shoot weight \pm SD as a function of plant age ($n = 10$). The difference in the weight is significant at 6 and 8 weeks of growth (Student's *t* test $P < 0.05$). **C**, Transmission electron microscopy images, showing chloroplast ultrastructure, were recorded at an age of 28 d of growth. Bar = $2 \mu\text{m}$.

in isolated thylakoid membranes has previously been attributed to an increased dissipation of H^+ gradient across thylakoids and uncoupled photophosphorylation (McCarty, 1980; Thomasset et al., 1984). Therefore, our results may indicate a higher H^+ gradient existing across the thylakoid membrane in the mutant compared to the wild type. The activities of the whole

linear electron transport chain were indistinguishable, based on the rates of oxygen consumption in the presence of methyl viologen (and sodium azide; Table I; Supplemental Table S1). Furthermore, no significant differences were found in the rates of cyclic electron transport based on the calculated half-time ($t_{1/2}$) for the P_{700}^+ re-reduction in darkness (Table I; Supplemental Table S1). Finally, the rates of CO_2 fixation were similar in *taac* and wild-type leaves (Supplemental Fig. S4) and are therefore not able to explain the reduced biomass of the mutant.

The leaves of wild-type and *taac* plants exhibited a typical O-J-I-P fluorescence induction curve (Supplemental Fig. S5; Strasser et al., 1996; Tsimilli-Michael et al., 2000). The shape of the curve, the values obtained for the relative variable fluorescence at the J-step (F_j) between 0.36 and 0.47, and the initial slope (M_0) between 0.78 and 1.26 are typical for healthy plants (Tsimilli-Michael et al., 2000). The analysis of the O-J-I-P curves allows the determination of the fate of the absorbed energy (parameter ABS): part of the excitation energy is dissipated in the antenna of the light-harvesting complex II (LHCII; parameter DI_0) as heat and/or fluorescence, and the remaining is channeled to the reaction centers (parameter TR_0). There, the energy is converted to redox energy by reducing the first stable quinone electron acceptor Q_A , while the reaction center (RC) Chl P_{680} is oxidized, thus creating an electron transport (parameter ET_0) within the photosynthetic apparatus (Supplemental Fig. S6). Table II compares the PSII behavior in wild-type and *taac* leaves using energy fluxes expressed per RC of the sample. The ABS/RC parameter was shown to be a measure of the antenna size (Strasser et al., 1996). The obtained similar values in *taac* and the wild type are in line with the absence of significant difference in the Chl *a/b* ratio (Table I) and the only slight modification in the Chl and xanthophyll levels (see below). Furthermore, calculations of the flux of energy reaching the RCII (TR_0) and of the flux of energy dissipated as heat and/or fluorescence in the antenna, when the first excitons closed all the RCII (DI_0) indicated no significant differences between the two types of plants (Table II). Taken together, these data indicate a similar distribution of energy fluxes at PSII level.

Table I. Photosynthetic characteristics of wild-type *Arabidopsis Ws* ecotype and *taac* plants grown at an irradiance of $120 \mu\text{mol photons m}^{-2} \text{s}^{-1}$. The parameters measured on 42-d-old plants were expressed as means \pm SD. *, Significantly different from the wild type (Student's *t* test $P = 0.001$).

Strain	Leaf Chlorophyll Content			Oxygen Evolution ^a			$t_{1/2} \text{ P}_{700}^+ \text{ s (n = 3)}^b$
	$\mu\text{g mg}^{-1}$ (n = 12–18)	$\mu\text{g cm}^{-2}$ (n = 12–18)	<i>a/b</i> (n = 12–18)	$\mu\text{mol O}_2 \text{ mg Chl}^{-1} \text{ h}^{-1}$			
				pPBQ (n = 4–6)	pPBQ + NH_4Cl (n = 2–4)	MV (n = 2–4)	
<i>Ws</i>	2.85 ± 0.18	42.26 ± 4.14	3.84 ± 0.07	133.0 ± 6.9	145.0 ± 7.5	-123.6 ± 14.8	1.8 ± 0.3
<i>taac</i>	2.79 ± 0.19	40.30 ± 1.94	3.91 ± 0.12	132.0 ± 6.7	$172.1 \pm 14.8^*$	-121.1 ± 0.3	2.1 ± 0.4

^aLight-saturated rate of oxygen evolution measured in thylakoid membranes in the presence of 0.5 mM phenyl-*p*-benzoquinone (pPBQ) without or with the addition of 10 mM NH_4Cl (uncoupler) or in the presence of 100 μM methyl viologen (MV) and 5 mM sodium azide. ^bCyclic electron transport was measured as half-time ($t_{1/2}$) for P_{700}^+ re-reduction.

Table II. Comparison of energy fluxes in the wild-type (*Ws*) and *taac* plants

Fast kinetics of fluorescence induction were recorded, and various energy fluxes were calculated per RC, as described in Supplemental Materials and Methods S1. ABS, absorption; TR_0 , trapping; DI_0 , dissipation; ET_0 , electron transport. Experiments are means \pm SD of 10 to 11 replicates. No significant differences were found between the two types of plants (Student's *t* test $P \geq 0.07$).

Energy Flux	<i>Ws</i>	<i>taac</i>
ABS/RC	2.815 \pm 0.065	2.607 \pm 0.074
TR_0 /RC	2.198 \pm 0.270	2.125 \pm 0.520
DI_0 /RC	0.624 \pm 0.192	0.483 \pm 0.024
ET_0 /RC	1.182 \pm 0.044	1.182 \pm 0.097

Nonphotochemical quenching of Chl fluorescence (*NPQ*) is an important photoprotective mechanism minimizing the photooxidative damage to the photosynthetic apparatus (for review, see Horton et al., 2008). To test whether the deficiency of TAAC affects photoprotection, the kinetics of *NPQ* formation were recorded for 20 min at photosynthetic active radiation (PAR) of 300, 600, and 1,250 $\mu\text{mol m}^{-2} \text{s}^{-1}$ in the two *taac* mutants and the respective background plants (Fig. 2; Supplemental Fig. S3C). The initial phase was transient with *NPQ* reaching a maximum 120 to 200 s after the first saturating pulse, as described by D'Haese et al. (2004). Nevertheless, the amplitude of this phase and the rate of *NPQ* formation were higher in *taac* mutants at the three tested light intensities. The second phase during the remaining illumination period of 20 min was slow and displayed no significant differences in the levels of *NPQ* between the mutants and the respective wild-type ecotype. The induced *NPQ* component was rapidly reversible and decayed during the dark period with similar kinetics and extent in the wild-type and *taac* plants (Fig. 2). Taken together, these results indicate that the mutants are more efficient in activating the formation of *NPQ*. Although of different ecotypes, the *SAIL_209_A12* mutant showed phenotypes identical with *FLAG_443D03* (Supplemental Fig. S3), chosen for detailed physiological and biochemical characterization (see below).

PSII Activity under High Light Conditions

The wild-type *Ws* and *FLAG_443D03 taac* plants were grown under GL conditions for 28 d and then under high light (HL; 950 $\mu\text{mol photons m}^{-2} \text{s}^{-1}$) conditions for additional 28 d, maintaining the diurnal cycle. Leaf samples were collected in the course of their growth to measure the maximum quantum yield of PSII photochemistry (F_v/F_m). Similar values (0.8) during day 0 of HL growth, followed by a slow decrease until day 4 (0.72), were measured in both types of plants (Fig. 3A). This parameter continued to decrease until day 7 in the mutant (0.62), whereas at the same time point the wild-type plants almost fully restored their PSII activity (0.78). The mutant fully

restored the activity only on day 14 (0.8). Taken together, the pattern observed for F_v/F_m indicates an enhanced susceptibility to high light for the mutant compared to the wild type. The slower recovery of PSII activity was at the expense of plant growth since the mutant displayed poor health, as shown in Figure 3B photos, taken after 28 d of HL conditions.

Leaf Pigment Analysis and Xanthophyll Cycle

The amplitude of the initial rapid phase of *NPQ* formation depends on the accumulation of H^+ in the thylakoid lumen and on the pigment and protein composition of the antenna (Horton et al., 2008). Acidification of the lumen leads to activation of violaxanthin de-epoxidase, which converts violaxanthin to antheraxanthin and finally to zeaxanthin as part of the xanthophyll cycle (for review, see Hieber et al., 2000; Horton et al., 2008). To investigate the mechanism behind the faster response of the mutant when it comes to *NPQ* (Fig. 2), we analyzed the wild-type and

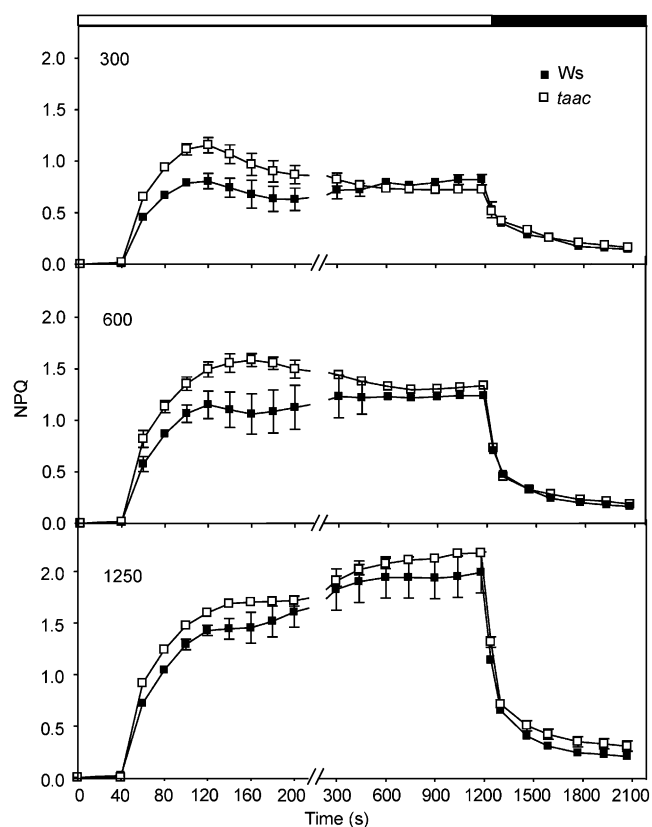


Figure 2. Kinetics of *NPQ* formation. Chlorophyll fluorescence of leaves detached from 16-h dark-adapted wild-type (*Ws*) and *taac* plants was recorded during a 20-min exposure to light (white bar) of 300, 600, or 1,250 $\mu\text{mol photons m}^{-2} \text{s}^{-1}$, followed by 15-min recovery in darkness (black bar). Saturating pulses (1.0 s) of actinic light were applied to determine the maximum fluorescence yield F_m or F_m' . *NPQ* was calculated from fluorescence data as $(F_m - F_m')/F_m'$ and plotted \pm SD as a function of illumination time ($n = 7-10$).

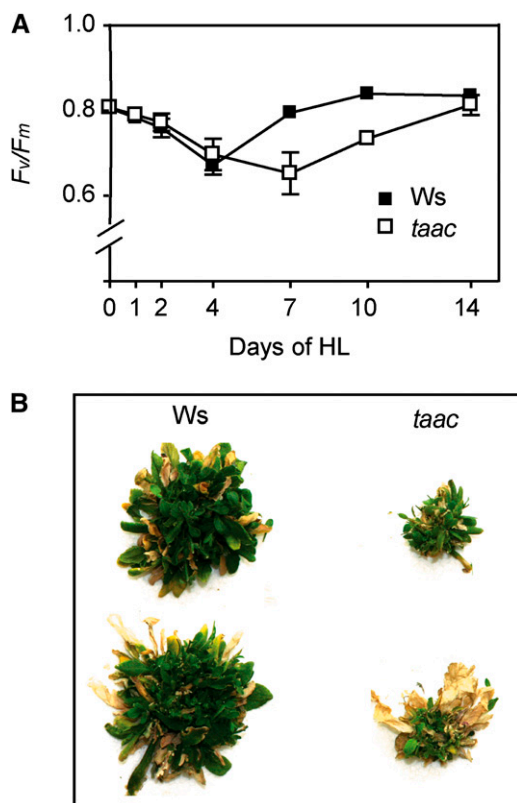


Figure 3. Photosynthetic characteristics of *taac* and wild-type plants of the same ecotype (Ws) grown under HL ($950 \mu\text{mol photons m}^{-2} \text{s}^{-1}$) conditions. Seedlings were germinated and grown initially at an irradiance of $120 \mu\text{mol photons m}^{-2} \text{s}^{-1}$. After 28 d, the plants were transferred in HL conditions for additional 28 d. A, The maximum quantum yield of PSII was measured as Chl fluorescence (F_v/F_m) after the 8-h light period and following 15-min dark period and plotted as a function of number of days in HL. The data plotted are means \pm SD (10–12 leaves from two to three independent experiments). B, Appearance of plant health during growth under HL conditions. Individual plants were photographed after the additional 28 d of growth under HL conditions.

taac plants in terms of pigment composition and interconversion of the xanthophylls, measured as de-epoxidation ratio.

Pigment analysis (neoxanthin, violaxanthin, lutein-5,6-epoxide, antheraxanthin, lutein, zeaxanthin, Chl *b*, Chl *b'*, Chl *a*, Chl *a'*, pheophytin *a*, and β -carotene) was performed from the leaves of the two types of plants, and the composition was found typical for healthy green leaves (Schoefs et al., 1996). The most abundant pigments were lutein, Chl *a*, and Chl *b* (Fig. 4A). Lutein-5,6-epoxide and Chl epimers were only present in traces and therefore were not quantified. Generally, the pigments were slightly but less abundant in the *taac* than in the wild-type leaves. At a PAR of $120 \mu\text{mol photons m}^{-2} \text{s}^{-1}$, the xanthophyll cycle was only weakly activated in both the wild type and mutant, as indicated by the low values of the de-epoxidation ratio (Fig. 4B). As PAR intensity increased, the xanthophyll cycle was progressively activated, and nota-

bly, to a much higher extent in the mutant than in the wild type. The de-epoxidation reaction saturated at approximately $1,250 \mu\text{mol photons m}^{-2} \text{s}^{-1}$ in the wild type but not in the *taac* leaves.

NPQ induction results from an excess of light at the level of PSII. It involves a response to the trans-thylakoid pH gradient, the xanthophyll cycle, the PsbS protein, and other, yet undefined aspects of photoinhibition. It has been postulated that the structural unit of NPQ consists of LHCII proteins and the PsbS protein and is formed upon protonation and binding of xanthophyll cycle carotenoids (Horton et al., 2008). Therefore, it was of great interest to examine the effect of nigericin and dithiothreitol (DTT), the well-known inhibitors of the trans-thylakoid pH gradient and of violaxanthin de-epoxidation, respectively. As shown in Figure 4C, in nigericin-treated leaves, the NPQ no longer displayed two phases but a continuous and weak increase with the increase of light intensity. The kinetics between the *taac* and wild-type plants were undistinguishable. Notably, DTT-treated leaves still display an initial rapid phase of NPQ formation. Like in control-treated leaves, both the amplitude and the rate of induction of this phase are higher in the *taac* mutant, whereas the steady-state NPQ levels are similar to the wild type. Since the relative amounts of PsbS and LHCII proteins were similar in the two types of plants (see below), these results collectively suggest that the trans-thylakoid pH gradient is the major factor responsible for the higher efficiency of NPQ formation observed in *taac* plants (Fig. 2).

Levels of Thylakoid Photosynthetic Proteins and PSII Phosphoproteins

Reduced weight was observed for fully developed *taac* plants grown under GL conditions. It was therefore tested whether the deficiency of TAAC changes the protein content in isolated thylakoid membranes. Western-blot analysis was performed using antibodies directed against various proteins of the PSII complex (CP43, D1, D2, PsbO, PsbP, Lhcb1, Lhcb2, and PsbS) as well as representative proteins in the ATP synthase (β -subunit of CF1) and the PSI complex (PsaA/B). Based on visual inspection of the western blots, no differences in the levels of analyzed proteins were apparent in *taac* compared to the wild-type thylakoids (Fig. 5A).

Phosphorylation of PSII proteins is an important step in the repair cycle of the complex (Tikkanen et al., 2008). To test whether the steady-state phosphorylation levels of PSII proteins were affected in the *taac* mutant, we isolated thylakoids from plants, which were dark adapted for 16 h or illuminated for 3 h either with GL or HL, and performed western blotting using an antiphosphothreonine antibody (Lundin et al., 2007b, and refs. therein). Under all three tested conditions, the levels of immunodetected phosphorylation of the PSII core proteins and the LHCII proteins were similar between the *taac* and wild-type thylakoids (Fig.

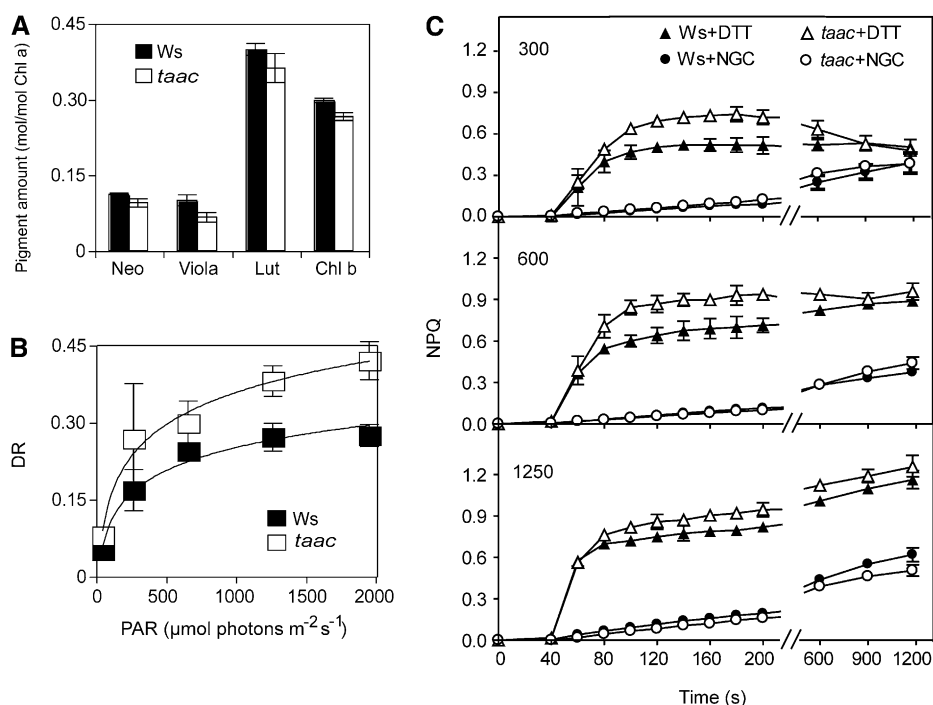


Figure 4. Pigment composition and xanthophyll cycle in Ws ecotype plants and the *taac* mutant. **A**, Leaves from plants grown at an irradiance of $120 \mu\text{mol photons m}^{-2} \text{s}^{-1}$ were detached at the end of the dark period, and the pigment composition was determined by HPLC. Amounts of main pigments are expressed relative to Chl *a* \pm *sd* ($n = 17$). **B**, Leaves were illuminated with PAR of intensities ranging between 53 and $1,952 \mu\text{mol photons m}^{-2} \text{s}^{-1}$. The time of illumination was 20 min for PAR intensities $< 1,000 \mu\text{mol photons m}^{-2} \text{s}^{-1}$ and reduced to 10 min for higher PAR intensities. Following illumination, pigments were extracted and analyzed by HPLC. Activity of the xanthophyll cycle was determined as de-epoxidation ratio (DR) \pm *sd* ($n = 3-4$ for each point). DR = (antheraxanthin + zeaxanthin)/(antheraxanthin + zeaxanthin + violaxanthin). **C**, Effect of nigericin and DTT on the kinetics of NPQ formation. Prior recording kinetics as described in Figure 2, plants were vacuum infiltrated with $50 \mu\text{M}$ nigericin (NGC) or 5 mM DTT. The curves for control leaves (infiltrated with water) were similar to those presented in Figure 2 and therefore are not shown here.

5B). These results indicate that depletion of TAAC does not influence the activity of thylakoid-associated PSII kinases and phosphatases.

Susceptibility to Photoinhibition of PSII

The reduced tolerance of the *taac* mutant during growth under HL conditions (Fig. 3) prompted us to test whether TAAC depletion influences the D1 protein degradation step during repair of PSII complex. To this end, the leaves detached from the *taac* and wild-type plants were illuminated for 1 and 3 h in the absence and presence of lincomycin, which blocks the synthesis of chloroplast-encoded proteins, including D1. The F_v/F_m parameter, used to monitor the maximal PSII activity, was recorded from intact leaves, whereas western blotting of isolated thylakoids with anti-D1 antibodies was performed to follow the D1 protein levels. When the wild-type and *taac* leaves were illuminated with GL in the absence or presence of lincomycin, no dramatic difference in the decay of F_v/F_m was observed (Fig. 6A). As expected, when protein synthesis was inhibited with lincomycin during the HL treatment, the PSII RCs of the wild type turned out

to be more prone to photodamage, as revealed by a faster decrease in the F_v/F_m parameter. Notably, under the HL conditions, the PSII RCs of *taac* were inactivated with similar rates in the absence and presence of lincomycin and to a similar extent (50%) as in the wild type in the presence of lincomycin. The D1 protein degradation was found blocked in all studied conditions in the mutant compared to the wild type where a clear loss of the protein was observed during both GL and HL in the presence of lincomycin (Fig. 6B). When PSII activity was measured in 3 h HL-treated leaves in the absence of lincomycin during subsequent 80 min of incubation in darkness, F_v/F_m was partially restored in the wild type (0.73), but slower and to a much lower extent in the mutant (0.59; Fig. 6C), supporting the malfunction in the PSII repair. Next, we preilluminated leaves for various periods of time at HL, allowed 5 min dark adaptation, and subsequently recorded NPQ induction curves at $1,250 \mu\text{mol photons m}^{-2} \text{s}^{-1}$ (Supplemental Fig. S7). The steady-state levels of NPQ were reached within 60 s of illumination in both wild-type and the mutant leaves (data not shown) and similarly decreased (Supplemental Fig. S7). Taken together,

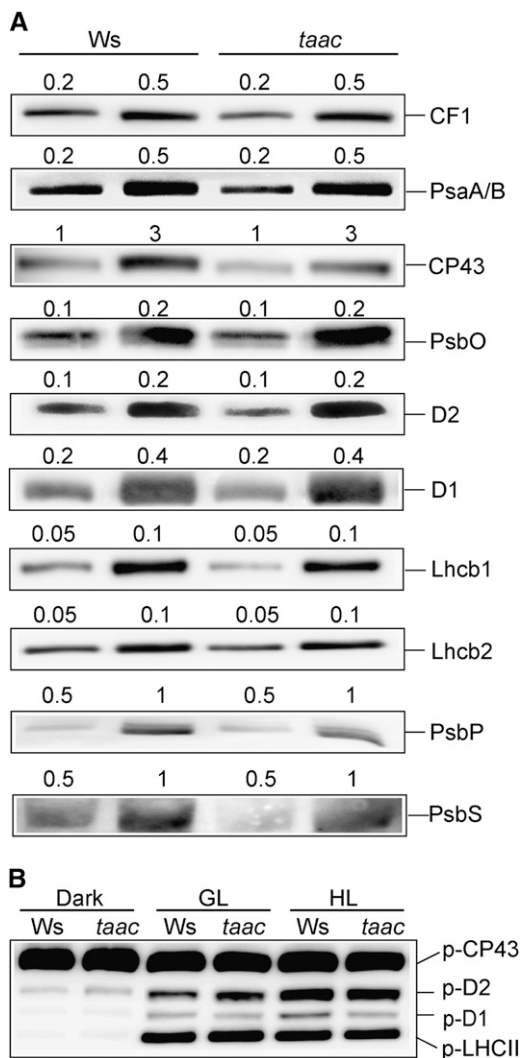


Figure 5. Analysis of photosynthetic proteins in wild-type (Ws) and *taac* plants. **A**, Thylakoid membranes were isolated from plants grown at an irradiance of $120 \mu\text{mol photons m}^{-2} \text{s}^{-1}$. Representative blots with antibodies against various photosynthetic proteins are shown. The loaded amount of Chl (μg) is indicated above each lane. **B**, Phosphorylation of PSII proteins was assessed in thylakoid membranes isolated in the presence of 10 mM NaF . Dark samples represent thylakoid membranes isolated from plants after 16 h in darkness. GL and HL samples are thylakoids isolated from plants exposed for 3 h to light of 120 and $950 \mu\text{mol photons m}^{-2} \text{s}^{-1}$, respectively. Representative western blot with antiphosphothreonine antibody from Cell Signaling is shown. The gels were loaded with $0.25 \mu\text{g}$ of Chl in each well. The positions of the major phosphorylated PSII proteins are indicated.

these data indicate that the *taac* plants are more susceptible than the wild type to high light, since the repair of PSII is malfunctioning in *taac* plants, while the photoprotection capacity does not differ between the two types of plants.

Leaves from plants exposed for 3 h to HL also have been studied in terms of chloroplast ultrastructure using electron microscopy (Fig. 6D). The dynamic structure of the grana can be dismantled and re-

formed, during the processes known as destacking and restacking, on a timescale of minutes (for review, see Anderson et al., 2008). Notably, the mutant retained slightly, but significantly, higher grana than their respective ecotype plants (i.e. approximately 6 versus 5 appressed thylakoid lamellae per granum on average). The granum length was also slightly, but significantly, longer in the mutant than in its respective ecotype (0.54 ± 0.15 and $0.51 \pm 0.15 \mu\text{m}$, respectively). When compared with the electron microscopy data obtained at GL conditions (Fig. 1C), it is obvious that HL treatment has induced destacking of grana and a decrease in granum length, but this process appeared to be partially inhibited in the mutant. The higher stacking in the mutant could be a protective mechanism against the effects of excess light and could also prevent access of proteases to the damaged D1 protein in PSII complexes unable to repair, as recently reported (Fristedt et al., 2009).

Organization of PSII Complexes

To explain the inability to degrade D1 in photo-inactivated PSII, we tested whether the deficiency of TAAC has an impact on the organization of PSII complexes in plants grown under GL and HL conditions. Thylakoids were isolated and solubilized mildly with detergent (dodecyl β -D-maltoside), and the various types of Chl protein complexes were separated by Blue-Native gel electrophoresis (BN-PAGE; Supplemental Fig. S8A). Western blotting with anti-D1 antibody identified four types of PSII subcomplexes: PSII-LHCII supercomplexes, PSII core dimers, PSII core monomers, and CP43-less monomers (Supplemental Fig. S8B). As revealed by quantification data presented in Table III, approximately 50% and 65% of the PSII complexes were found as monomers (sum of PSII core and CP43-less monomers) in wild-type and *taac* plants grown under GL conditions, respectively. Notably, the PSII supercomplexes were clearly less abundant in *taac* plants, indicating that PSII is already inhibited under GL conditions and requires repair. CP43-less PSII monomers represent the form that accumulates under conditions of intensive PSII repair, including D1 degradation (Rokka et al., 2005). Indeed, the mutant forms more CP43-less monomers with respect to the wild type, but the ratio to PSII core monomers is quite similar in the two types of plants (6:2 and 5:1, respectively). When grown under HL conditions, the PSII monomers dominated over the dimers in both types of plants, i.e. approximately 85% monomers were detected. Despite this, the wild-type plants accumulated the largest amounts of CP43-less monomers (20%) compared to the mutant (6%). The calculated ratio of 13:1 for PSII core monomers to CP43-less monomers in *taac* compared to 3:1 in the wild type indicates a poor dissociation of CP43 from the PSII monomer in *taac* plants during repair.

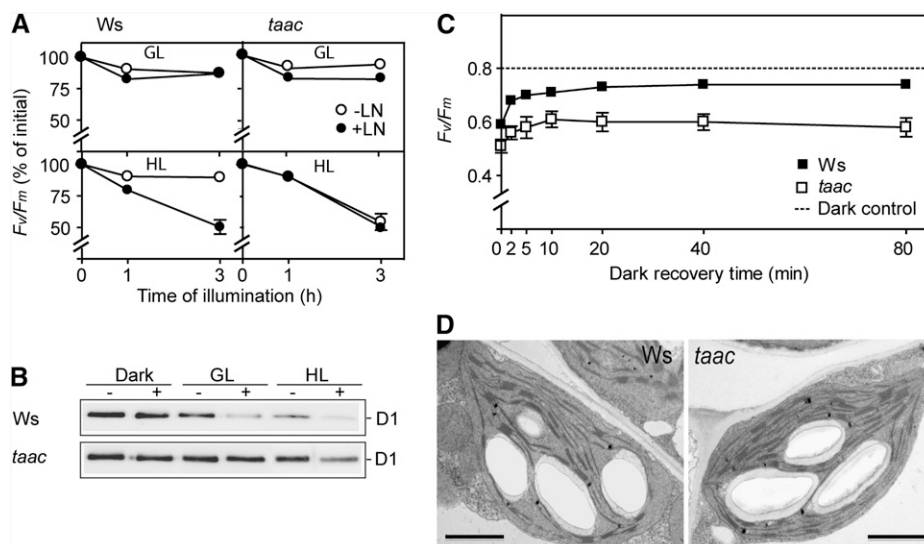


Figure 6. Susceptibility of wild-type (Ws) and *taac* plants to photoinhibition of PSII. Leaves detached from plants grown at an irradiance of GL ($120 \mu\text{mol photons m}^{-2} \text{s}^{-1}$) were exposed to GL or HL ($950 \mu\text{mol photons m}^{-2} \text{s}^{-1}$) treatments in the presence (+) or absence (-) of lincomycin (LN) for 1 and 3 h. A, Chl fluorescence was measured in leaves after 5 min dark adaptation, and the F_v/F_m parameter was calculated. The relative levels of F_v/F_m were plotted \pm sd as a function of illumination time ($n =$ two to three independent experiments). B, Representative western blots with anti-D1 of thylakoids from the 3-h light treatment ($0.25 \mu\text{g Chl/lane}$). C, Chl fluorescence was measured in leaves following 3 h of HL treatment in the absence of lincomycin and incubated in darkness for the indicated periods of time. The values obtained for the F_v/F_m parameter were plotted \pm sd ($n =$ two independent experiments). D, Transmission electron microscopy images of chloroplast ultrastructure from 3-h HL-treated plants. Bar = $2 \mu\text{m}$.

DISCUSSION

Arabidopsis contains an ATP/ADP carrier in the chloroplast thylakoid membrane, named TAAC. Its high expression levels under high light stress conditions (Thuswaldner et al., 2007), which primarily induce an inactivation of the PSII complex in the thylakoid membrane, pointed to a role of TAAC in the turnover of this complex. In this study, we employed a combination of biochemical, physiological, and electron microscopy approaches to investigate two *taac* mutant lines. Although the mutants were from two different collections and ecotypes, their phenotype was similar, emphasizing the specific effect of the mutation. We show that depletion of TAAC results in reduced plant growth. The mutants display

wild-type levels of photosynthetic pigments, proteins, and activities. Therefore, the reduced growth must be a physiological consequence of TAAC depletion and its impact on the PSII repair cycle, more specifically impairment of CP43 dissociation from the complex, a step preceding the proteolytic degradation of the D1 protein. We also show that in the absence of TAAC, a higher trans-thylakoid electrochemical H^+ gradient is used in the first minutes of illumination to induce transiently higher NPQ levels, which relaxes when reaching steady state levels.

The distinct response of PSII complexes to high light stress in the wild type and *taac* plants is likely to provide information about the physiological role of the TAAC protein by supplying nucleotides in the thylakoid lumen. The deficiency of TAAC increases the

Table III. Organization of PSII complexes in wild-type (Ws) and *taac* plants

Plants were grown for 21 d in GL ($120 \mu\text{mol photons m}^{-2} \text{s}^{-1}$) and then transferred for additional 14 d to GL or HL ($950 \mu\text{mol photons m}^{-2} \text{s}^{-1}$). The proportional amount (%) of each type of PSII subcomplex in each type of plant and condition was determined from D1 protein western blots of Blue Native gels as in Supplemental Figure S8. Based on these levels, the ratio of PSII core monomer to CP43-less monomer was calculated. The presented values are average of three independent experiments. nd, Not detected.

Type of PSII Subcomplex	GL		HL	
	Ws	<i>taac</i>	Ws	<i>taac</i>
PSII-LHCII supercomplex	26	11	nd	nd
PSII core dimer	24	23	17	15
PSII core monomer	43	55	63	79
PSII core CP43-less monomer	7	12	20	6
PSII core monomer: CP43-less monomer	6:1	5:1	3:1	13:1

susceptibility of PSII to photoinhibition (Figs. 3 and 6). The inhibition of D1 protein degradation results in the malfunctioning of the repair cycle. The site of malfunction was localized at the step when CP43 dissociates from damaged PSII, since a relatively low proportion of CP43-less monomers were detected in the mutant compared with the wild type, and most complexes were found as intact core monomers (Table III; Supplemental Fig. S8).

Interestingly, the phenotype of a T-DNA insertion line lacking the PsbO2 protein (*psbo2*) resembles *taac* with respect to PSII repair during HL stress. The *psbo2* mutant displays smaller size and reduced HL stress tolerance, impaired D1 protein degradation, and predominance of the core monomer over the CP43-less monomer (Lundin et al., 2007b, 2008). This raises the question whether the poor dissociation of the CP43 subunit from the PSII core monomer observed in *taac* and *psbo2* plants is due to a cross talk between TAAC and PsbO2 in performing ATP transport and GTPase-mediated signaling, resulting in efficient turnover of the D1 protein. The following lines of experimental evidence support this hypothesis. (1) D1 protein degradation following PSII photoinactivation is a GTP-dependent process (Spetea et al., 1999). (2) PsbO is a GTPase and dissociates from PSII complex in a light- and GTP-dependent manner (Lundin et al., 2007a). PsbO is present in PSII core monomers but not in CP43-less monomers (Rokka et al., 2005), indicating that its dissociation precedes that of CP43. (3) Arabidopsis PsbO2 is a better GTPase than PsbO1. Its elimination leads to accumulation of PSII core monomers and impaired repair cycle (Lundin et al., 2007b, 2008). (4) TAAC depletion leads to a reduced trans-thylakoid ATP transport and conversion to GTP in the lumen (Thuswaldner et al., 2007) as well as to accumulation of PSII core monomers and impaired repair cycle (this study). Interaction of TAAC with PSII proteins is not documented, and its function is most likely to supply nucleotides to the lumen for PsbO2-mediated signaling of PSII disassembly.

Generally, the short-term photosynthetic acclimation of plants to high light includes reversible phosphorylation of thylakoid membrane proteins and the dissipation of excess excitation energy as heat. Based on our results, it appears that the former is functioning optimally in *taac* mutants, whereas the latter is more efficiently activated compared to the wild type. The PSII proteins were found similarly phosphorylated in *taac* and the wild type in both dark- and light-adapted plants (Fig. 5B). A similar phosphorylation pattern was observed in the previously characterized *psbo2* mutant (Lundin et al., 2007b). This would imply that the responsible protein kinases and/or phosphatases require neither lumenal nucleotides supplied by TAAC nor GTPase-mediated signaling.

Regarding *NPQ*, the *taac* mutants were distinguishable from the respective wild-type ecotypes particularly in terms of rate and amplitude of the initial rapid phase of *NPQ* formation and also in terms of

activation of violaxanthin de-epoxidase (Figs. 2 and 4; Supplemental Fig. S3D). Notably, *psbo2* plants display similar *NPQ* induction and capacity as the wild type (Allahverdiyeva et al., 2009). This implies that the *NPQ* pattern observed in *taac* plants is not related to the impaired GTP-mediated PSII repair cycle during photoinhibition, but rather a physiological consequence of TAAC depletion.

Two relevant questions are whether and by which mechanism the deficiency of TAAC leads to a transient acidification of the lumen in the first minutes of illumination. In vivo measurements in wild-type and *taac* plants did not reveal significant differences in the electrochemical H^+ gradient (A. Kanazawa, D.M. Kramer, and C. Spetea, unpublished data). The cellular homeostasis, similar to that of the wild type, is most likely reached in the mutant in order to maintain steady and balanced electrochemical gradient across the thylakoid membrane. Nevertheless, there are several lines of evidence to support the establishment of a transiently higher trans-thylakoid H^+ gradient in the mutant: (1) an enhanced stimulatory effect of NH_4Cl on the rate of oxygen evolution from isolated thylakoids; (2) faster and higher amplitude of the initial rapid phase of *NPQ* formation in dark-adapted leaves, but not in preilluminated leaves (this pattern is preserved in DTT-treated, but not in nigericin-treated, leaves); (3) a higher de-epoxidation ratio and, thus, a more active violaxanthin de-epoxidase. The steady-state *NPQ* levels are indistinguishable between the wild type and mutants and are lowered drastically by nigericin and to a lower extent by treatment with DTT. Therefore, we cannot exclude that an important fraction of the observed *NPQ* is zeaxanthin independent. This will support previous and recent observations about zeaxanthin-independent *NPQ* mechanisms (Finazzi et al., 2004; Li et al., 2009; Lambrev et al., 2010). Thus, the transient accumulation of higher electrochemical H^+ gradient in the mutants more efficiently activates photoprotective xanthophyll cycle-dependent and -independent mechanisms compared to the wild type.

We do not understand at present stage the mechanism by which absence of TAAC leads to the above-discussed effects on H^+ gradient and photoprotection. An attractive possibility would be that trans-thylakoid adenine nucleotide exchange by TAAC is electrogenic (ATP^{4-}/ADP^{3-}), as demonstrated for the mitochondrial AAC-catalyzed transport (Gropp et al., 1999). Although AAC and TAAC share a similar structure and antiport mechanism (Thuswaldner et al., 2007), the electrogenic properties of TAAC activity dissipating a fraction of the H^+ gradient in the wild-type plants, while accumulating it in the *taac* mutants, remain to be investigated.

The results presented and discussed here support the previously proposed significant role of the thylakoid lumen in metabolism and cellular signaling. The thylakoid lumen is a multifunctional cellular compartment, as based on the large variety of proteins iden-

tified biochemically and by large-scale proteomics (Spetea and Thuswaldner, 2008). The TAAC protein and activity renders this view even more complex with respect to the regulation of PSII repair and photoprotection during light stress.

MATERIALS AND METHODS

Plant Material and Growth Conditions

The *taac* mutant is a T-DNA insertion knockout Arabidopsis (*Arabidopsis thaliana*) mutant for the TAAC gene (At5g01500; FLAG_443D03, Ws ecotype) obtained from PublicLines at Institut National de la Recherche Agronomique (<http://dbsgap.versailles.inra.fr/publiclines/>). PCR analysis was performed to confirm the homozygosity of the mutant, whereas the absence of the TAAC protein was verified by western blotting, as described (Thuswaldner et al., 2007). The Southern-blot analysis of *Hind*III-digested mutant performed with a T-DNA-specific probe demonstrated that the FLAG line contained only one T-DNA insert (Supplemental Fig. S1). The details of the Southern blotting are given in Supplemental Materials and Methods S1.

Arabidopsis seeds for the SAIL_209_A12 T-DNA insertion line for the TAAC gene (Columbia ecotype; Supplemental Fig. S2A) were produced by Syngenta (McElver et al., 2001) and ordered at the Salk SIGnAL T-DNA express Arabidopsis Gene mapping tool (<http://www.signal.salk.edu/cgi-bin/tdnaexpress>). PCR and RT-PCR analyses of this mutant are given in Supplemental Materials and Methods S1. Although of different ecotypes, the SAIL_209_A12 mutant showed visible phenotypes identical with FLAG_443D03, chosen for detailed physiological and biochemical characterization. Characterization of SAIL_209_A12 is presented in Supplemental Table S1 and Supplemental Figure S4.

The two mutants and wild-type Arabidopsis of respective ecotype were grown hydroponically at an irradiance of 120 $\mu\text{mol photons m}^{-2} \text{s}^{-1}$ (GL) at 22°C with 8-h-light/16-h-dark cycles and relative humidity 70% for 42 d unless otherwise indicated. For HL stress experiments, 28-d-old GL plants were grown at an irradiance of 950 $\mu\text{mol photons m}^{-2} \text{s}^{-1}$ (HL) for an additional 28 d. For pigment analysis, plants were grown on soil under GL conditions for 15 to 17 d before use. For analysis of PSII subcomplexes, plants were grown on soil for 21 d under GL conditions and then grown for additional 14 d under either GL or HL conditions.

Chlorophyll Fluorescence, Oxygen Evolution, P_{700} Oxidoreduction, and CO_2 Fixation

Chl fluorescence at room temperature was measured using a pulsed-amplitude fluorometer either dual PAM-100 (for the data presented in Table II and Supplemental Fig. S5) or model PAM-210 (Walz; for the data presented in Figs. 2, 3, and 6 and Supplemental Fig. S3). The maximum quantum yield of PSII photochemistry (F_v/F_m) was determined as a ratio of variable fluorescence (F_v) to maximal fluorescence (F_m) measured from attached leaves dark adapted for 15 min.

Fast kinetics of Chl fluorescence induction were recorded, and the obtained O-J-I-P transient was analyzed according to the JIP-test (Strasser et al., 1996). Using the fluorescence parameters, the energy fluxes per RC were calculated. For details and equations, see Supplemental Materials and Methods S1. All the measurements were performed on attached leaves dark adapted for 15 min.

During HL growth, the maximum quantum yield of PSII photochemistry was determined as Chl fluorescence (F_v/F_m) in leaves harvested after the 8-h light period followed by 15 min of dark adaptation. For determination of NPQ, slow kinetics of Chl fluorescence induction were recorded in leaves detached from 16 h dark-adapted plants, exposed for 20 min to PAR of 300, 600, and 1,250 $\mu\text{mol photons m}^{-2} \text{s}^{-1}$ followed by 15 min in darkness. Saturating pulses (1.0 s) of actinic light were applied to determine F_m or F_m' . Where indicated, 16-mm leaf discs were vacuum infiltrated with 5 mM DTT or 50 μM nigericin (Ruban and Horton, 1995; Johnson et al., 2008). The NPQ parameter was calculated using the equation $\text{NPQ} = (F_m - F_m')/F_m'$.

Steady-state oxygen evolution was measured with a Clark-type electrode (Chlorolab 2 system; Hansatech) in isolated thylakoid membranes using high-intensity red LED light (LH11/2R, 1,250 $\mu\text{mol photons m}^{-2} \text{s}^{-1}$) at 22°C and in the presence of 0.5 mM phenyl-*p*-benzoquinone as electron acceptor from PSII or 100 μM methyl viologen and 5 mM NaN_3 to measure the whole electron

transport chain. To uncouple the thylakoids, 10 mM NH_4Cl was added to the reaction mixture prior the measurement of oxygen evolution.

P_{700} redox changes were measured from intact leaves with JTS-10 (Biologic). P_{700} was oxidized by a far-red LED (720 nm) and computed as $\Delta I/I700 = \Delta I/I820\text{nm} - 0.8 \times \Delta I/I880\text{nm}$. The kinetics of P_{700}^+ rereduction in the dark was fitted by a single exponential term and the half-lifetimes calculated via $t_{1/2} = \ln 2 T$.

CO_2 fixation was measured from intact leaves using an open gas portable photosynthesis system (LI-6400; LI-COR) as described in Supplemental Materials and Methods S1.

Electron Microscopy

The plants used for ultrastructural investigations were 28 d old. The leaves were directly fixed at least 3 h after the start of the light phase and prepared for electron microscopy as described by Abdolkader et al. (2007). The ultrathin (70 nm) sections of the leaf CSs were investigated by a Hitachi 7100 transmission electron microscope at 75-kV accelerating voltage. From all samples at least 35 different plastids were studied (chosen randomly from at least 100 plastids), and representative pictures are shown. Calculations of plastid size and number of grana per plastid profile were done on 35 representative plastids. The granum height (number of appressed thylakoid lamellae) and length were calculated from analyzing 230 to 330 grana in each strain. Granum length was defined and measured at the middle of the granum.

Pigment Analysis

Chl content of whole leaves was determined by extraction in 96% ethanol and spectrophotometry according to Lichtenthaler and Wellburn, (1983). For determination of the xanthophyll cycle activity, the leaves were illuminated for 20 min with PAR of various intensities ranging between 53 and 1,952 $\mu\text{mol photons m}^{-2} \text{s}^{-1}$. Because long and intense illumination triggers pigment photodestruction, the time of illumination was reduced to 10 min for PAR intensity higher than 1,000 $\mu\text{mol m}^{-2} \text{s}^{-1}$, as recommended by Niyogi et al. (1998). When the illumination period was completed, Chl and carotenoids were extracted from detached leaves (Schoefs, 2002) and analyzed by HPLC (Darko et al., 2000). Details are provided in Supplemental Materials and Methods S1. The xanthophyll cycle or de-epoxidation ratio was measured as (antheraxanthin + zeaxanthin)/(antheraxanthin + zeaxanthin + violaxanthin).

Thylakoid Preparation

Thylakoid membranes were isolated from 16-h dark-adapted plants and purified as described (Norén et al., 1999). In some experiments aimed at studying the steady-state level of phosphorylation of PSII proteins, thylakoid membranes were isolated in the presence of 10 mM NaF (a general inhibitor of protein phosphatases) from plants that were dark adapted and exposed for 3 h to GL or HL. Chl concentration was determined spectrophotometrically in 80% acetone according to Porra et al. (1989).

Short-Term Light Treatment

In experiments aimed to study the effect of inhibition of chloroplast protein synthesis, detached leaves were treated with 2 mM lincomycin in darkness overnight. The leaves together with the media were then transferred to petri dishes and exposed to GL or HL for 1 and 3 h at 22°C. Chl fluorescence was measured in control and lincomycin-treated leaves after 5 min of dark adaptation. For quantification of D1 protein levels, the leaves were frozen in liquid nitrogen and stored at -80°C until isolation of thylakoid membranes. Where indicated, Chl fluorescence was recorded in 3 h HL-treated leaves during a subsequent period of recovery in darkness.

SDS-PAGE, BN-PAGE, and Western Blotting

Thylakoid proteins were separated by SDS-PAGE using 14% (w/v) acrylamide gels with 6 M urea. Following electrophoresis and electroblotting, various photosynthetic proteins were immunodetected using specific antibodies and the ECL-Plus detection system (GE Healthcare). Antibodies were raised in rabbit against PsaA/B, CP43, D2, D1, PsbO, and PsbP proteins from spinach (*Spinacia oleracea*). Antibodies against the CFI β -subunit of ATP-synthase, Lhcb1, Lhcb2, and PsbS proteins were purchased from Agrisera.

Where indicated, rabbit anti-phosphothreonine antibodies from Cell Signaling were used.

For determination of PSII subcomplex distribution, thylakoid membranes were isolated and solubilized as described (Lundin et al., 2008). The Chl protein complexes were separated by BN-PAGE, and the PSII complexes immunodetected with the anti-D1 antibody.

Statistical Analysis

The mean and SD were calculated for each data set, where appropriate. Standard error bars were plotted except where smaller than the symbol size. Where appropriate, the Student's *t* test was used to identify the difference between the wild type and the mutant.

Supplemental Data

The following materials are available in the online version of this article.

Supplemental Figure S1. Southern blot of the *EcoRI*-digested FLAG_443D03 *taac* mutant DNA probed with a radiolabeled T-DNA fragment.

Supplemental Figure S2. Screening for homozygous *Arabidopsis* SAIL_209_A12 *taac* mutant.

Supplemental Figure S3. Characterization of the SAIL_209_A12 *taac* knockout mutant.

Supplemental Figure S4. CO₂ fixation of the *taac* mutant and wild-type *Arabidopsis* Ws ecotype.

Supplemental Figure S5. Fast fluorescence kinetics of *taac* mutant and wild-type *Arabidopsis* Ws ecotype.

Supplemental Figure S6. A highly simplified model presenting the energy fluxes per RC in photosystem II.

Supplemental Figure S7. Steady-state levels of nonphotochemical quenching in high-light stressed leaves.

Supplemental Figure S8. Analysis by Blue Native gel electrophoresis (BN-PAGE) of protein complexes from wild-type and *taac* plants.

Supplemental Table S1. Photosynthetic characteristics of wild-type *Arabidopsis* of Columbia ecotype (Col) and SAIL_209_A12 *taac* plants.

Supplemental Materials and Methods S1.

ACKNOWLEDGMENTS

We thank the Institut National de la Recherche Agronomique (Station de Génétique, Versailles, France) and the *Arabidopsis* Biological Resource Center (The Ohio State University, Columbus, OH) for providing the T-DNA insertion lines FLAG_443D03 and SAIL_209_A12, respectively. We thank Csilla Jónás (Eötvös University, Budapest) for her skillful assistance with the electron microscopy sample preparation and Yagut Allahverdiyeva (University of Turku, Turku, Finland) for help with the cyclic electron transport measurements. We also thank the anonymous reviewers for their constructive comments and experiment suggestions.

Received March 5, 2010; accepted March 28, 2010; published March 31, 2010.

LITERATURE CITED

Abdelkader AF, Aronsson H, Solymosi K, Böddi B, Sundqvist C (2007) High salt stress induces swollen prothylakoids in dark-grown wheat and alters both prolamellar body conversion and reformation after irradiation. *J Exp Bot* **58**: 2553–2564

Allahverdiyeva Y, Mamedov F, Holmström M, Nurmi M, Lundin B, Styring S, Spetea C, Aro EM (2009) Comparison of the electron transport properties of the *psbo1* and *psbo2* mutants of *Arabidopsis thaliana*. *Biochim Biophys Acta* **1787**: 1230–1237

Anderson JM, Chow WS, De Las Rivas J (2008) Dynamic flexibility in the

structure and function of photosystem II in higher plant thylakoid membranes: the grana enigma. *Photosynth Res* **98**: 575–587

Aro EM, Suorsa M, Rokka A, Allahverdiyeva Y, Paakkari V, Saleem A, Battchikova N, Rintamäki E (2005) Dynamics of photosystem II: a proteomic approach to thylakoid protein complexes. *J Exp Bot* **56**: 347–356

Darko E, Schoefs B, Lemoine Y (2000) Improved liquid chromatographic method for the analysis of photosynthetic pigments of higher plants. *J Chromatogr* **876**: 111–116

D'Haese D, Vandermeiren K, Caubergs RJ, Guisez Y, De Temmerman L, Horemans N (2004) Non-photochemical quenching kinetics during the dark to light transition in relation to the formation of antheraxanthin and zeaxanthin. *J Theor Biol* **227**: 175–186

Finazzi G, Johnson GN, Dall'Osto L, Joliot P, Wollman FA, Bassi R (2004) A zeaxanthin-independent nonphotochemical quenching mechanism localized in the photosystem II core complex. *Proc Natl Acad Sci USA* **101**: 12375–12380

Fristedt R, Willig A, Granath P, Crèvecoeur M, Rochaix JD, Vener AV (2009) Phosphorylation of photosystem II controls functional macroscopic folding of photosynthetic membranes in *Arabidopsis*. *Plant Cell* **21**: 3950–3964

Gropp T, Brustovetsky N, Klingenberg M, Müller V, Fendler K, Bamberg E (1999) Kinetics of electrogenic transport by the ADP/ATP carrier. *Biophys J* **77**: 714–726

Hausühl K, Andersson B, Adamska I (2001) A chloroplast DegP2 protease performs the primary cleavage of the photodamaged D1 protein in plant photosystem II. *EMBO J* **20**: 713–722

Hieber AD, Bugos RC, Yamamoto HY (2000) Plant lipocalins: violaxanthin de-epoxidase and zeaxanthin epoxidase. *Biochim Biophys Acta* **1482**: 84–91

Horton P, Johnson MP, Perez-Bueno ML, Kiss AZ, Ruban AV (2008) Photosynthetic acclimation: does the dynamic structure and macro-organisation of photosystem II in higher plant grana membranes regulate light harvesting states? *FEBS J* **275**: 1069–1079

Johnson MP, Davison PA, Ruban AV, Horton P (2008) The xanthophyll cycle pool size controls the kinetics of non-photochemical quenching in *Arabidopsis thaliana*. *FEBS Lett* **582**: 262–266

Kapri-Pardes E, Naveh L, Adam Z (2007) The thylakoid lumen protease Deg1 is involved in the repair of photosystem II from photoinhibition in *Arabidopsis*. *Plant Cell* **19**: 39–47

Lambrev PH, Nilkens M, Miloslavina M, Jahns P, Holzwarth AR (2010) Kinetic and spectral resolution of multiple nonphotochemical quenching components in *Arabidopsis* leaves. *Plant Physiol* **152**: 1611–1624

Li Z, Ahn TK, Avenson TJ, Ballottari M, Cruz JA, Kramer DM, Bassi R, Fleming GR, Keasling JD, Niyogi KK (2009) Lutein accumulation in the absence of zeaxanthin restores nonphotochemical quenching in the *Arabidopsis thaliana npq1* mutant. *Plant Cell* **21**: 1798–1812

Lichtenthaler HK, Wellburn AR (1983) Determinations of total carotenoids and chlorophylls *a* and *b* of leaf extracts in different solvents. *Biochem Soc Trans* **603**: 591–592

Lindahl M, Spetea C, Hundal T, Oppenheim AB, Adam Z, Andersson B (2000) The thylakoid FtsH protease plays a role in the light-induced turnover of the photosystem II D1 protein. *Plant Cell* **12**: 419–431

Lundin B, Hansson M, Schoefs B, Vener AV, Spetea C (2007b) The *Arabidopsis* PsbO2 protein regulates dephosphorylation and turnover of the photosystem II reaction centre D1 protein. *Plant J* **49**: 528–539

Lundin B, Nurmi M, Rojas-Stuetz M, Aro EM, Adamska I, Spetea C (2008) Towards understanding the functional difference between the two PsbO isoforms in *Arabidopsis thaliana*—insights from phenotypic analyses of *psbo* knockout mutants. *Photosynth Res* **98**: 405–414

Lundin B, Thuswaldner S, Shutova T, Eshaghi S, Samuelsson G, Barber J, Andersson B, Spetea C (2007a) Subsequent events to GTP binding by the plant PsbO protein: structural changes, GTP hydrolysis and dissociation from the photosystem II complex. *Biochim Biophys Acta* **1767**: 500–508

McCarty RE (1980) Delineation of the mechanism of ATP synthesis in chloroplasts: use of uncouplers, energy transfer inhibitors, and modifiers of coupling factor 1. *Methods Enzymol* **69**: 719–728

McElver J, Tzafirir I, Aux G, Rogers R, Ashby C, Smith K, Thomas C, Schetter A, Zhou Q, Cushman MA, et al (2001) Insertional mutagenesis of genes required for seed development in *Arabidopsis thaliana*. *Genetics* **159**: 1751–1763

Nelson N, Ben-Shem A (2004) The complex architecture of oxygenic photosynthesis. *Nat Rev Mol Cell Biol* **5**: 971–982

- Norén H, Svensson P, Andersson B** (1999) Auxiliary photosynthetic functions of *Arabidopsis thaliana*—studies *in vitro* and *in vivo*. *Biosci Rep* **19**: 499–509
- Niyogi KK, Grossman AR, Björkman O** (1998) *Arabidopsis* mutants define a central role for the xanthophyll cycle in the regulation of photosynthetic energy conversion. *Plant Cell* **10**: 1121–1134
- Porra RJ, Thompson WA, Kriedemann PE** (1989) Determination of accurate extinction coefficients and simultaneous-equations for assaying chlorophyll *a* and chlorophyll *b* extracted with 4 different solvents—verification of the concentration of chlorophyll standards by atomic absorption spectroscopy. *Biochim Biophys Acta* **975**: 384–394
- Rokka A, Suorsa M, Saleem A, Battchikova N, Aro EM** (2005) Synthesis and assembly of thylakoid protein complexes: multiple assembly steps of photosystem II. *Biochem J* **388**: 159–168
- Ruban AV, Horton P** (1995) An investigation of the sustained component of nonphotochemical quenching of chlorophyll fluorescence in isolated chloroplasts and leaves of spinach. *Plant Physiol* **108**: 721–726
- Ruiz Pavón L, Lundh E, Lundin B, Mishra A, Persson BL, Spetea C** (2008) *Arabidopsis* ANTR1 is a thylakoid Na(+)-dependent phosphate transporter: functional characterization in *Escherichia coli*. *J Biol Chem* **283**: 13520–13527
- Schoefs B** (2002) Chlorophyll and carotenoid analysis in food products. Properties of the pigments and methods of analysis. *Trends Food Sci Technol* **13**: 361–371
- Schoefs B, Lemoine Y, Bertrand M** (1996) Reversed-phase high-performance liquid chromatography separation of photosynthetic pigments and their precursors. *Am Biotechnol Lab* **14**: 18–22
- Silva P, Thompson E, Bailey S, Kruse O, Mullineaux CW, Robinson C, Mann NH, Nixon PJ** (2003) FtsH is involved in the early stages of repair of photosystem II in *Synechocystis sp PCC 6803*. *Plant Cell* **15**: 2152–2164
- Spetea C, Hundal T, Lohmann E, Andersson B** (1999) GTP bound to chloroplast thylakoid membranes is required for light-induced, multi-enzyme degradation of the photosystem II D1 protein. *Proc Natl Acad Sci USA* **96**: 6547–6552
- Spetea C, Hundal T, Lundin B, Heddad M, Adamska I, Andersson B** (2004) Multiple evidence for nucleotide metabolism in the chloroplast thylakoid lumen. *Proc Natl Acad Sci USA* **101**: 1409–1414
- Spetea C, Schoefs B** (2010) Solute transporters in plant thylakoid membranes—key players during photosynthesis and stress. *Commun Integr Biol* **3**: 1–8
- Spetea C, Thuswaldner S** (2008) Update in nucleotide-dependent processes in plant chloroplasts. In B Schoefs, ed, *Plant Cell Compartments: Selected Topics*. Research Signpost, Kerala, India, pp 105–149
- Strasser RJ, Eggenberg P, Strasser BJ** (1996) How to work without stress but with fluorescence. *Bull Soc R Sci Liège* **65**: 330–349
- Thomasset B, Barbotin JN, Thomas D** (1984) The effects of oxygen solubility and high concentrations of salts on photosynthetic electron transport in chloroplast membranes. *Biochem J* **218**: 539–545
- Thuswaldner S, Lagerstedt JO, Rojas-Stütz M, Bouhidel K, Der C, Leborgne-Castel N, Mishra A, Marty F, Schoefs B, Adamska I, Persson BL, Spetea C** (2007) Identification, expression, and functional analyses of a thylakoid ATP/ADP carrier from *Arabidopsis*. *J Biol Chem* **282**: 8848–8859
- Tikkanen M, Nurmi M, Kangasjärvi S, Aro EM** (2008) Core protein phosphorylation facilitates the repair of photodamaged photosystem II at high light. *Biochim Biophys Acta* **1777**: 1432–1437
- Tsimilli-Michael M, Eggenberg P, Biro B, Köves-Oechy K, Vörös I, Strasser RJ** (2000) Synergetic and antagonistic effects of arbuscular mycorrhizal fungi and *Azospirillum* and *Rhizobium* nitrogen-fixers on the photosynthetic activity of Alfalfa, probed by the polyphasic chlorophyll *a* fluorescence transient O-J-I-P. *Appl Soil Ecol* **15**: 169–182